Journal of Physics: Conference Series

PAPER • **OPEN ACCESS**

Initial Sticking Coefficient Attenuation of Gases in Carbon Monoxide Sensing on $Pt_{80}Au_{14}Ti_6$

To cite this article: R Marjunus 2019 *J. Phys.: Conf. Ser.* **1338** 012021

View the article online for updates and enhancements.

IOP ebooks™

Bringing you innovative digital publishing with leading voices to create your essential collection of books in STEM research.

Start exploring the collection - download the first chapter of every title for free.

This content was downloaded from IP address 125.162.107.6 on 04/11/2019 at 10:26

IOP Conf. Series: Journal of Physics: Conf. Series **1338** (2019) 012021 doi:10.1088/1742-6596/1338/1/012021

Initial Sticking Coefficient Attenuation of Gases in Carbon Monoxide Sensing on $Pt_{80}Au_{14}Ti_6$

R Marjunus

University of Lampung, Jl. Prof. Dr. Soemantri Brodjonegoro No.1, Bandar Lampung 35145, Indonesia

roniyus.1977@fmipa.unila.ac.id

Abstract. It has been proved that $Pt_{80}Au_{14}Ti_6$ can give proper signals as a CO sensitive layer in air at room temperature. Unfortunately, there is no signal anymore from this sample, if it is kept in air more than 24 hours. To overcome this problem, we carried out dry etching technic. The atmosphere testing also has been done in technic etcher chamber by keeping the samples separately in Ar, N_2, CO, and O_2 with pressure 1 atm for 24 hours without taking out the samples after etching process from the chamber. These experiments found that oxygen causes this loss signal problem. Oxygen can diffuse up to 170 Angstrom under the Pt surface to be subsurface oxygen. This diffusion changes the surface structure of Pt(100)(1x1) to hex-Pt(100) which impacts the attenuating of the initial sticking coefficient of gases. Simulations which have been conducted in this research produced the attenuating factor, i.e., $1 - 0.00585 \exp(5.76664 O_{sub})$, where O_{sub} is the concentration of subsurface oxygen.

1. Introduction

Carbon monoxide (CO) is a gas species which is present in the earth atmosphere with a natural concentration of less than 0.001 % [1]. CO is also produced by human activities such as from vehicles, fires, explosions and cigarette smoking. Especially in a fire accident, CO is always created as a first product due to incomplete combustion of hydrocarbon [1]. Above a concentration of 30 ppm, CO is toxic to human health [2]. On the other hand, CO is colorless and odorless. Therefore, a sensor is needed to detect the existence of CO, to provide a warning on a dangerous level of CO to the human being, CO emission control for an internal combustion engine, etc.

A good sensor is a sensor that has four ”high” and three ”low” criteria, i.e., high sensitivity, high selectivity, high stability, high signal/noise ratio, low power consumption, low weight and low price [3]. These criteria are being tried to be achieved in gas sensor’s world using some categories of gas sensors. Among the many existing categories of gas sensors, one of them is solid state sensor. Two subtypes of the solid state sensor are resistance based sensors and work function change based sensors [4]. There are disadvantages of resistance based sensors [5], i.e.:

1. It cannot use metal as the sensitive material because metal has low resistivity.
2. It cannot detect neither chemisorbed nor weakly bound physisorbed species at ambient up to slightly elevated temperatures.
3. Heating is required. If there are some sensitive layers used at room temperature, normally it will be compensated with the high of the gas concentration. It means criteria as a good sensor, i.e., high sensitivity, is not satisfied. In the case for CO sensor, some reports which claim their sensitive

Content from this work may be used under the terms of the Creative Commons Attribution 3.0 licence. Any further distribution of this work must maintain attribution to the author(s) and the title of the work, journal citation and DOI.
Published under licence by IOP Publishing Ltd

material can be used at room temperature but only for high CO concentration such as at 100 ppm [6], 500 ppm [7], 1000 ppm [8][9], and 20000 ppm [10].
4. Elevated temperatures imply high power consumption.

Instead of facing the disadvantages of resistance based sensor, the second subtype of solid state sensor can be an alternative. It is field effect gas sensor or work function change based sensor [4], which needs a Floating Gate Field Effect Transistor (FGFET) as the transducer [3]. Some advantages of work function change based sensor [5] are:
1. It can use a wide variety of sensitive materials.
2. It can detect both chemisorbed and weakly bound physisorbed species at ambient up to slightly elevated temperatures.
3. Heating is not obligatory.
4. Low power consumption.
5. Freedom in choice of sensing material [11]

Many materials can be used as a candidate for a CO sensitive layer, one of them is platinum (Pt). Since 1922, Pt-CO and Pt-O interactions were known by Langmuir [12]. Pt as a sensing material was used as a detection layer in work function change based sensor, e.g., for ozone [13] or hydrogen [14]. It was also applied as a catalyst on Ga_2O_3 semiconductor work function change based sensors to decrease the operation temperature as a CO sensor to near room temperature [15], while metal oxides such as Ga_2O_3 and SnO_2 can only be used at high operation temperatures [16]. Even though Pt can decrease the operation temperature of metal oxide CO sensors but pure Pt is already known not good as CO sensitive layer in work function change based sensor, as reported by Leu et al. [17]. They obtained the average work function change 60 mV for 1000 ppm, 1700 ppm, and 2500 ppm CO in the air at room temperature. Although it was achieved at room temperature, it could not be applied for allowed maximum CO concentration in a workplace, i.e., 30 - 35 ppm. It was also tried to mix Pt with other metal such Cu which had been performed by Kiss et al., [18]. Kiss et al. reported Pt (<1 nm) which was sputtered on Cu plate (1 cm^2) then annealed at 200^{o}C for 1 hour in air could give work function change 6 mV (with good back response) for 2000 ppm CO at room temperature. The Pt/Cu layer was also able exhibiting work function change until 55 mV after the layer was heat-treated at 200^{o}C for 2 hours in air, but the signals had a very small back response (2 mV). Then, other metal which has a chance also to be mixed with Pt is gold (Au). Investigation of CO interaction with Au was known since 1925 by Bone and Andrew [19]. Researches about the interaction of Pt-CO and Au-CO also have been done by many researchers, e.g., by Ertl et al. [20]. Not only interaction of pure Pt or pure Au with CO which was studied, but the interaction of PtAu alloy with CO was also investigated such by Bouwman and Sachtler by using photoelectric work function determination in 1970 [21]. Bouwman and Sachtler reported no significant work function change of Au, while Pt and other alloys such as $Pt_{84}Au_{16}$ showed a work function change of about 0.04 eV in 10^{-5} - 10^{-4} Torr CO in a vacuum chamber at ambient temperature after one day. Though report of Bouwman and Sachtler was promising, it is needed improvement in the normal air because their experiment had been done in vacuum condition. Besides regarded the response of PtAu alloy to CO, Simon et al. also reported that $Pt_{90}Au_{10}$ can detect CO in the hydrogen atmosphere as a work function change based sensor [22]. As the report of Bouwman and Sachtler, and the information from Simon et al. should also be tested in normal air at room temperature because the PtAu alloy in their report was used in the hydrogen atmosphere.

Marjunus (2014) reported that $Pt_{80}Au_{14}Ti_6$ samples with 5 nm Ti as adhesive layer is also able to give good signals to 30, 60, and 120 ppm of CO in air with Relative Humidity (*RH*) = 42% at room temperature (25^{o}C) as presented in figure 1 [23].

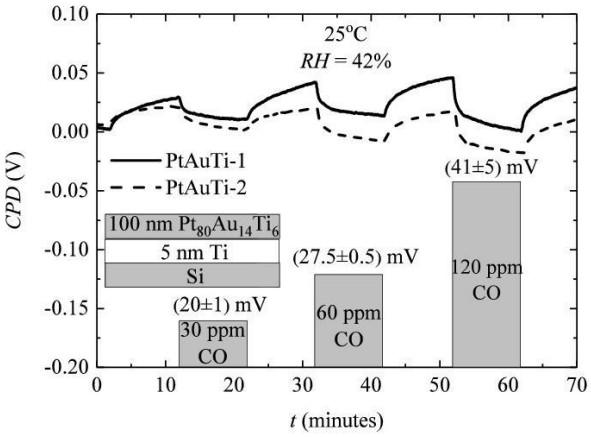

Figure 1. The CPD signals of $Pt_{80}Au_{14}Ti_6$ samples with 5 nm Ti as adhesive layer to 30, 60, and 120 ppm of CO in air with *RH* = 42% at room temperature (25°C) [23].

Although $Pt_{80}Au_{14}Ti_6$ can give good signals as a CO sensitive layer, unfortunately there is no signal anymore from these PtAuTi samples if they are kept in air for long time, e.g. 7 months (figure 2) [23].

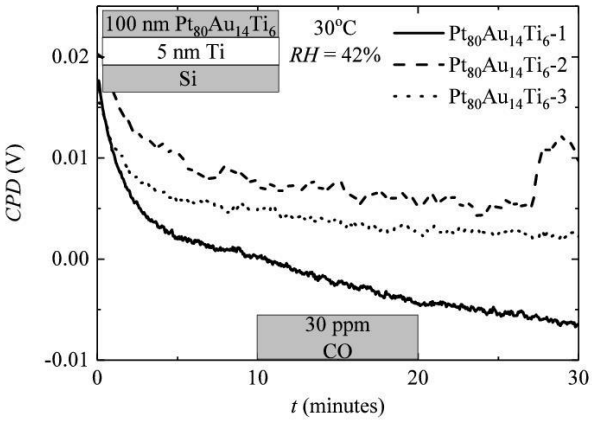

Figure 2. Signals of $Pt_{80}Au_{14}Ti_6$ samples with 5 nm Ti as adhesive layer to 30 ppm of CO in air with *RH* = 42% at room temperature (30◦C) after 7 months produced [23].

To find the way how to refresh the samples, etching the samples by Technic Planar Etcher II AMPEL Nanofabrication Facility had been tried. The etching rate is about 0.5 nm/minute. After the samples were etched in argon plasma with 300 W, base pressure 5×10^{-2} mbar, and working pressure 2.6×10^{-1} mbar, for 20 minutes, samples can give their responses as before. But, when the samples are kept in air for 24 hours in Technic Planar Etcher II chamber, there is no response anymore to CO pulses, it has been proved for three times on three $Pt_{80}Au_{14}Ti_6$ samples. To find out the root of this problem, the atmosphere testing with Ar, N_2, CO and O_2 have been done. The atmosphere testing was done in technic etcher chamber by keeping the samples with a specific gas without taking out the samples after etching process from the chamber then keeping the gas flow for 24 hours (it means the pressure chamber was always 1 atm). The results from this test show that the samples still can give their responses at room temperature (30°C) after they were etched in argon plasma with 300 W, base pressure 5×10^{-2} mbar, and working pressure 2.6×10^{-1} mbar, for 20 minutes then kept them either in Ar, N_2 or CO atmosphere with pressure

1 atm for 24 hours but there is no response anymore when they are kept in O_2. It proves that oxygen causes this problem. It has been proved for three $Pt_{80}Au_{14}Ti_6$ samples [23].

Oxygen is suspected playing behind the lost signal phenomenon. It is supported by some scientific reports, started by Schmiedl et al. who reported that oxygen is detected at a level significantly above the noise, up to 170 Angstrom under the Pt surface [24]. It occurs because oxygen can diffuse from the surface of Pt as chemisorbed oxygen to under the Pt surface as subsurface oxygen [25], with its diffusion constant $D = 10^{-19}$ cm^2/s. The diffusion process from chemisorbed oxygen to be subsurface oxygen changes the Pt(100) structure from (1x1)-phase to hex-phase as illustrated in figure 3(a) and (b) [26].

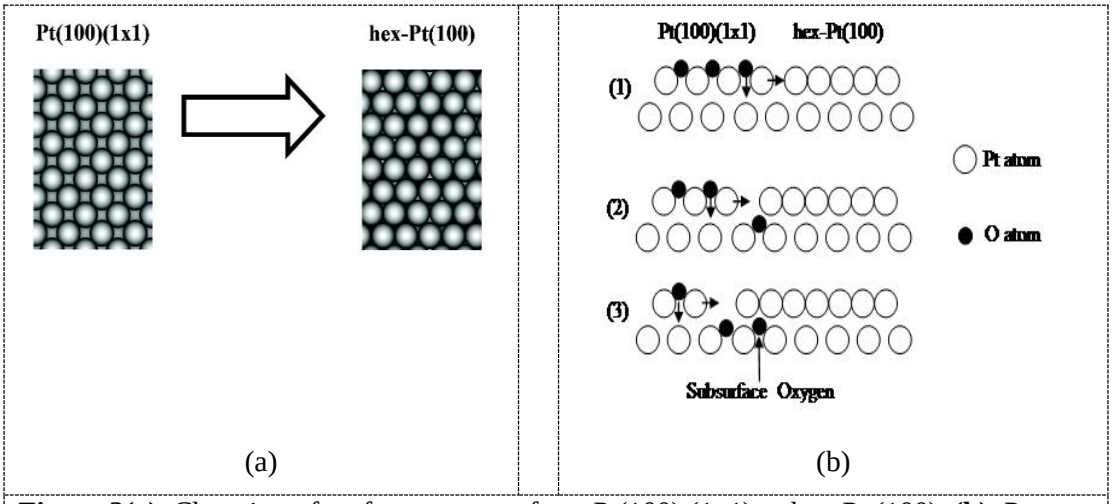

Figure 3(a). Changing of surface structure from Pt(100) (1x1) to hex-Pt (100). **(b).** Process of chemisorbed oxygen to be subsurface oxygen [26].

The concentration of subsurface oxygen will attenuate the value of initial sticking coefficient. In order to calculate the attenuation of the initial sticking coefficient, a reaction mechanism model is built based on its state of the art. Many articles had reported regarding the interaction between CO and Pt. It is started from the Ph.D. Thesis of Callaghan [27]. Callaghan reported that many reactions were already reported regarding the kinetics and catalysis of the Water-Gas-Shift Reaction (WGS). The WGS reaction as given in Equation 1.

$$CO + H_2O \rightleftharpoons H_2 + CO_2 \quad (1)$$

This reaction provides a method for extracting the energy from the toxic CO by converting it into usable H_2 along with CO_2 which can be tolerated by the fuel cell. Although Water-Gas-Shift Reaction only occurs at high-temperature range (350ºC – 600ºC) or low-temperature range (150ºC – 300ºC) not at room temperature, the chemical reactions which are used in Callaghan's thesis are important to be used in this research, to complete all of the reaction possibilities. Perhaps, some reactions are not necessary, but simulation will decide it whether some reactions are essential or not. According to Callaghan, there were already 60 reactions which were reported by the scientists. From all reactions, only 18 reactions which were adopted by Callaghan for WGS reaction, because of some reasons [27]. The reactions are as presented in table 1.

This research uses also Reaction No. 45/Equation 2, Reaction No. 45/Equation 3 and other reaction which is also important i.e. Equation 4,

$$O_2{}^{(g)} + 2S \rightleftharpoons 2O^{(s)} \quad (2)$$

$$OH^{(g)} + S \rightleftharpoons OH^{(s)} \quad (3)$$

$$CO^{(s)} \rightleftharpoons C^{(s)} + O^{(s)} \quad (4)$$

Table 1. Water-gas shift reactions mechanisms, filtered by Callaghan [27]

No.	Reaction
1.	$CO^{(g)} + S \rightleftharpoons CO^{(s)}$
2.	$H_2O^{(g)} + S \rightleftharpoons H_2O^{(s)}$
3.	$H_2O^{(s)} + S \rightleftharpoons OH^{(s)} + H^{(s)}$

No	Reaction
4.	$CO^{(s)} + O^{(s)} \rightleftharpoons {CO_2}^{(s)} + S$
5.	$CO^{(s)} + OH^{(s)} \rightleftharpoons HCOO^{(s)} + S$
6.	$OH^{(s)} + S \rightleftharpoons O^{(s)} + H^{(s)}$
7.	$CO^{(s)} + OH^{(s)} \rightleftharpoons {CO_2}^{(s)} + H^{(s)}$
8.	$HCOO^{(s)} + S \rightleftharpoons {CO_2}^{(s)} + H^{(s)}$
9.	$HCOO^{(s)} + O^{(s)} \rightleftharpoons {CO_2}^{(s)} + OH^{(s)}$
10.	$H_2O^{(s)} + O^{(s)} \rightleftharpoons 2OH^{(s)}$
11.	$H_2O^{(s)} + H^{(s)} \rightleftharpoons OH^{(s)} + {H_2}^{(s)}$
12.	$OH^{(s)} + H^{(s)} \rightleftharpoons O^{(s)} + {H_2}^{(s)}$
13.	$HCOO^{(s)} + OH^{(s)} \rightleftharpoons {CO_2}^{(s)} + H_2O^{(s)}$
14.	$HCOO^{(s)} + H^{(s)} \rightleftharpoons {CO_2}^{(s)} + {H_2}^{(s)}$
15.	${CO_2}^{(s)} \rightleftharpoons {CO_2}^{(g)} + S$
16.	$H^{(s)} + H^{(s)} \rightleftharpoons {H_2}^{(s)} + S$
17.	${H_2}^{(s)} \rightleftharpoons {H_2}^{(g)} + S$
18.	$2H^{(s)} \rightleftharpoons {H_2}^{(g)} + 2S$

Then, in order to calculate the coverage change rate of a gas on a surface in ad sorption process (r_a in atoms/s or molecules/s), it is started from the rate of adsorption, as given in Equation 5, as follows [28],

$$r_a = \frac{dN_{ads}}{dt} \tag{5}$$

where N_{ads} is the amount of adsorbed atoms or molecules on the surface which can be defined as in Equation 6,

$$N_{\text{ads}} = \sigma\Theta \tag{6}$$

where σ is the surface atom density of the layer (atoms/m^2) and Θ is the coverage of the gas on the sample surface (in mono layer or ML). On the other hand, r_a depends on the incident molecular flux (F, in molecules.m^{-2}s^{-1}) which is called Hertz-Knudsen Law [29], as given by Equation 7,

$$F = \frac{P}{\sqrt{2\pi mkT}}. \tag{7}$$

and the sticking probability (S, dimensionless) which is exhibited in Equation 8,

$$S = S_0(1-\theta)^2 \exp\left(-\frac{E_a}{kT}\right) \tag{8}$$

where P is partial pressure of the gas (in Pa), m is mass of the gas molecule (in kg), k is Boltzmann constant = 1.38×10^{-23} JK^{-1}, T is temperature (in K), S_0 is initial sticking coefficient or sticking coefficient when the coverage is still zero (dimensionless), and z is factor 1 for undissociated gas and 2 for

dissociated gas. If Equation 5 – 8 are combined, it is obtained the coverage change rate of a gas on a surface in adsorption process as shown in Equation 9,

$$\frac{d\theta}{dt} = \frac{S_0(1-\theta)^2}{\sqrt{2\pi mkT}} \exp\left(-\frac{E_a}{kT}\right). \tag{9}$$

When an adsorbed atom or molecule gas A reacts with an adsorbed atom or molecule of gas B on the surface to be molecule AB, based on the Langmuir-Hinshelwood mechanism, the coverage change rate of AB can be calculated as given in Equation 10, [30][31],

$$\frac{d\theta_{AB}}{dt} = \nu_r \exp\left(-\frac{E_r}{kT}\right)\theta_A\theta_B \tag{10}$$

where ν_r is the pre-exponential factor/Arrhenius coefficient which determines the frequency of reaction A and B (in reaction/s), E_r is activation energy of reaction between atom/molecule gas A and B (in eV), Θ_A and Θ_B are the coverage of gas A dan gas B respectively (dimensionless).

Then, if an adsorbed molecule gas (e.g. AB) dissociates into A and B, the coverage change rate of A can be calculated as presented in Equation 11 [31],

$$\frac{d\theta_A}{dt} = \nu_{diss} \exp\left(-\frac{E_d}{kT}\right)\theta \tag{11}$$

where ν_{diss} is the pre-exponential factor/Arrhenius coefficient which determines the frequency of AB dissociation (in dissociation/s), E_{diss} is activation energy of gas AB dissociation (in eV) and Θ_{AB} is the coverage of molecule AB (dimensionless).

Afterward, when an adsorbed atom or molecule will be desorbed, the coverage change rate the atom or molecule on the sample surface can be calculated as revealed in Equation 12 [31],

$$\frac{d\theta}{dt} = \nu_d \exp\left(-\frac{E_d}{kT}\right)\theta \tag{12}$$

where ν_d is the pre-exponential factor/Arrhenius coefficient which determines the frequency of desorption (desorption/s).

2. Data/Materials and Methods

The concentration of subsurface oxygen can be calculated using diffusion equation which is given in Equation 13 [32],

$$\frac{\partial\theta}{\partial t} = D\nabla^2 C \tag{13}$$

Equation 13 will be solved with numerical method for one dimension as given in Equation 14,

$$C_{i,j+1} = C_{i,j} + D\Delta t\left(\frac{C_{i+1} - 2C_{ij} + C_{i,-1,j}}{\Delta y^2}\right) \tag{14}$$

Then, the simulation calculates the amount of O_{chem} and O_{sub} in Mono Layer (ML) with/without considering the surface reaction (adsorption, reaction, and desorption). Considering/not considering the surface reaction are aimed to know whether there is a significant role or not of the surface reaction, or which is responsible for the amount of O_{chem} and O_{sub}.

Afterward, experiments for 24 hours on $Pt_{80}Au_{14}Ti_6$ with 5 nm Ti as adhesive layer to 30 ppm which are exposed to CO in air with *RH* = 42% at room temperature (30°C) after etched in argon plasma with 300 W with base pressure 5×10^{-2} mbar, and working pressure 2.6×10^{-1} mbar would be done. The Signal

Attenuation (*SA*) would be formulated as percentage of the signal to the initial signal. Afterward, the data of *SA* from these experiments were plotted together with the result from experiment.

3. Results and Discussion

The model in this research uses the Callaghan's reaction (Reaction No. 1 - 18 in table 1) and Equation 1 – 3. Then, based on (a) all reactions, (b) the coverage change rate of a gas on a surface in adsorption process (Equation 9), (c) the coverage change rate of reaction between element A and B (Equation 10), (d) the coverage change rate of dissociation AB (Equation 11) and (e) the coverage change rate the desorbed atom or molecule on the sample surface (Equation 12), it can be developed the Surface Coverage Differential Equations for Θ_{CO}, Θ_{O}, Θ_{CO2}, Θ_{H2O}, Θ_{OH}, Θ_{H}, Θ_{HCOO}, Θ_{H2} and Θ_{C} as presented in Equation 15 – 23,

$$\frac{d\Theta_{CO}}{dt} = r_{f1}F_{CO} - r_{f4}\Theta_{CO}\Theta_{O} + r_{r4}\Theta_{CO_2} - r_{f5}\Theta_{CO}\Theta_{OH} + r_{r5}\Theta_{HCOO} - r_{f7}\Theta_{CO}\Theta_{H} + r_{r7}\Theta_{CO_2}\Theta_{H} - r_{f61}\Theta_{CO} + r_{r61}\Theta_{C}\Theta_{O} - r_{r1}\Theta_{CO} \tag{15}$$

$$\frac{d\Theta_{O}}{dt} = 2r_{f45}F_{O_2} - r_{f4}\Theta_{CO}\Theta_{O} + r_{r4}\Theta_{CO_2} + r_{f6}\Theta_{OH} - r_{r6}\Theta_{O}\Theta_{H} - r_{f9}\Theta_{HCOO}\Theta_{O} + r_{r9}\Theta_{CO_2}\Theta_{OH} - r_{f10}\Theta_{H_2O}\Theta_{O} + r_{r10}\Theta_{OH}^{\ 2} + r_{f12}\Theta_{OH}\Theta_{H} - r_{r12}\Theta_{O}\Theta_{H_2} + r_{f61}\Theta_{CO} - r_{r61}\Theta_{C}\Theta_{O} - 2r_{r45}\Theta_{O}^{\ 2} \tag{16}$$

$$\frac{d\Theta_{CO_2}}{dt} = r_{r15}F_{CO_2} + r_{f4}\Theta_{CO}\Theta_{O} - r_{r4}\Theta_{CO_2} + r_{f7}\Theta_{CO}\Theta_{H} - r_{r7}\Theta_{CO_2}\Theta_{H} + r_{f8}\Theta_{HCOO} - r_{r8}\Theta_{CO_2}\Theta_{H} + r_{f9}\Theta_{HCOO}\Theta_{O} - r_{r9}\Theta_{CO_2}\Theta_{OH} + r_{f13}\Theta_{HCOO}\Theta_{OH} - r_{r13}\Theta_{CO_2}\Theta_{H_2O} + r_{f14}\Theta_{HCOO}\Theta_{H} - r_{r14}\Theta_{CO_2}\Theta_{H_2} - r_{f9}\Theta_{HCOO}\Theta_{O} + r_{r9}\Theta_{CO_2}\Theta_{OH} - r_{f15}\Theta_{CO_2} \tag{17}$$

$$\frac{d\Theta_{H_2O}}{dt} = r_{f2}F_{H_2O} - r_{f3}\Theta_{H_2O} + r_{r3}\Theta_{OH}\Theta_{H} - r_{f10}\Theta_{H_2O}\Theta_{O} + r_{r10}\Theta_{OH}^{\ 2} - r_{f11}\Theta_{H_2O}\Theta_{H} + r_{r11}\Theta_{OH}\Theta_{H_2} + r_{f13}\Theta_{HCOO}\Theta_{OH} - r_{r13}\Theta_{CO_2}\Theta_{H_2O} - r_{r2}\Theta_{H_2O} \tag{18}$$

$$\frac{d\Theta_{OH}}{dt} = r_{f46}F_{OH} + r_{f3}\Theta_{H_2O} - r_{r3}\Theta_{OH}\Theta_{H} - r_{f5}\Theta_{CO}\Theta_{OH} + r_{r5}\Theta_{HCOO} - r_{f6}\Theta_{OH} + r_{r6}\Theta_{O}\Theta_{H} - r_{f7}\Theta_{CO}\Theta_{H} + r_{r7}\Theta_{CO_2}\Theta_{H} + r_{f9}\Theta_{HCOO}\Theta_{O} - r_{r9}\Theta_{CO_2}\Theta_{OH} + 2r_{f10}\Theta_{H_2O}\Theta_{O} - 2r_{r10}\Theta_{OH}^{\ 2} + r_{f11}\Theta_{H_2O}\Theta_{H} - r_{r11}\Theta_{OH}\Theta_{H_2} - r_{f12}\Theta_{OH}\Theta_{H} + r_{r12}\Theta_{O}\Theta_{H_2} - r_{f13}\Theta_{HCOO}\Theta_{OH} + r_{r13}\Theta_{CO_2}\Theta_{H_2O} + r_{f8}\Theta_{HCOO} - r_{r8}\Theta_{CO_2}\Theta_{H} - r_{f46}\Theta_{OH} \tag{19}$$

$$\frac{d\Theta_{H}}{dt} = 2r_{r18}F_{H} + r_{f3}\Theta_{H_2O} - r_{r3}\Theta_{OH}\Theta_{H} + r_{f6}\Theta_{OH} - r_{r6}\Theta_{O}\Theta_{H} + r_{f7}\Theta_{CO}\Theta_{H} - r_{r7}\Theta_{CO_2}\Theta_{H} + r_{f8}\Theta_{HCOO} - r_{r8}\Theta_{CO_2}\Theta_{H} - r_{f11}\Theta_{H_2O}\Theta_{H} + r_{r11}\Theta_{OH}\Theta_{H_2} - r_{f12}\Theta_{OH}\Theta_{H} + r_{r12}\Theta_{O}\Theta_{H_2} - r_{f14}\Theta_{HCOO}\Theta_{H} + r_{r14}\Theta_{CO_2}\Theta_{H_2} - r_{f16}\Theta_{H}^{\ 2} + r_{r16}\Theta_{H_2} - 2r_{f18}\Theta_{H}^{\ 2} \tag{20}$$

$$\frac{d\Theta_{HCOO}}{dt} = r_{f5}\Theta_{CO}\Theta_{OH} - r_{r5}\Theta_{HCOO} - r_{f8}\Theta_{HCOO} + r_{r8}\Theta_{CO_2}\Theta_{H} - r_{f9}\Theta_{HCOO}\Theta_{O} + r_{r9}\Theta_{CO_2}\Theta_{OH} - r_{f13}\Theta_{HCOO}\Theta_{OH} + r_{r13}\Theta_{CO_2}\Theta_{H_2O} - r_{f14}\Theta_{HCOO}\Theta_{H} + r_{r14}\Theta_{CO_2}\Theta_{H_2} \quad (21)$$

$$\frac{d\Theta_{H_2}}{dt} = r_{r17}F_{H_2} + r_{f11}\Theta_{H_2O}\Theta_{H} - r_{r11}\Theta_{OH}\Theta_{H_2} + r_{f12}\Theta_{OH}\Theta_{H} - r_{r12}\Theta_{O}\Theta_{H_2} + r_{f14}\Theta_{HCOO}\Theta_{H} - r_{r14}\Theta_{CO_2}\Theta_{H_2} + r_{f16}\Theta_{H}{}^{2} - r_{r16}\Theta_{H_2} - r_{f17}\Theta_{H_2} \quad (22)$$

$$\frac{d\Theta_{C}}{dt} = r_{f61}\Theta_{CO} - r_{r61}\Theta_{C}\Theta_{O} \quad (23)$$

where

$$F_X = (1-\Theta_x)^2 \frac{P}{\sigma\sqrt{2\pi mkT^c}} \quad (24)$$

where X in F_x the symbol of the gas, n is 1 or 2 for undissociated or dissociated gas respectively, P is partial pressure of the gas (Pa) and m is the atom mass of the gas (kg), k is Boltzmann constant, T is temperature (in K) and σ is surface density of atom on the sensitive layer surface (surface density of Pt, Au and Ti are 1.3×10^{19} atoms/m^2, 1.2×10^{19} atoms/m^2 and 2.3×10^{19} atoms/m^2 respectively) [23]. Afterward, in Equation 15 – 23, it is found also reaction rate ($r_{f\text{ or }r,N}$) where

$$r_{f\text{ or }r,N} = \nu_{r\text{ or }r,N}\ \exp\left(-\frac{E_{r\text{ or }r,N}}{kT}\right) \quad (25)$$

where subscript f, r and N in $r_{f\text{ or }r,N}$ mean forward reaction, reverse reaction and number of reaction respectively, $\nu_{r\text{ or }r,N}$ is Arrhenius Coefficient (s^{-1}) and $E_{r\text{ or }r,N}$ is activation energy (eV) [31]. There is an exception of Equation 25 for forward Reaction No. 1, 2, 15, 17, 18, 45 and 46 as given in Equation 26 [31],

$$r_{f,N} = S_{0x}\ \exp\left(-\frac{E_{f,N}}{kT}\right) \quad (26)$$

where S_{0X} in $r_{f,N}$ is the initial sticking coefficient of gas X. Afterward, since the sensitive layer is a mixture of more than one material, the total of gas atom/molecule coverage on the surface is proposed as given in Equation 27,

$$\frac{d\Theta_j}{dt} = \sum_{i=Pt}^{Ti} \%i \frac{d\Theta_{ji}}{dt} \quad (27)$$

where j is index for the element symbol of the gas, %i is the percentage of Pt, Au or Ti on the sample and $\frac{d\Theta_{ji}}{dt}$ is the coverage rate of every gas which is already given in Equation 15 – 23. The coverage of every gas will be found in the simulation from Equation 27. Then, the work function of the sensitive layer during exposed with the gases is determined as function of the gas coverages in Equation 28,

$$\Phi(\Theta) = \sum_{i=Pt}^{Ti} \sum_{j=CO}^{C} \%i\Phi_{ji}(\Theta_i) \quad (28)$$

where $\Phi_{ji}(\theta_{ji})$ is the work function of gas j on material i as already given in Marjunus (2018) [23]. Finally, the CPD is calculated by substituting $\Phi(\theta)$ which is obtained from Equation 28 to Equation 29 [23],

$$CPD \approx \frac{\Phi_S}{|e|} \tag{29}$$

where $|e|$ is the elementary charge.

Then, experiments for 24 hours on $Pt_{80}Au_{14}Ti_6$ with 5 nm Ti as adhesive layer to 30 ppm which are exposed to CO in air with *RH* = 42% at room temperature (30°C) after etched in argon plasma with 300 W with base pressure 5×10^{-2} mbar, and working pressure 2.6×10^{-1} mbar, has been done as presented in figure 4. According to the figure 4, the average signals show that the signal of samples attenuates by the time.

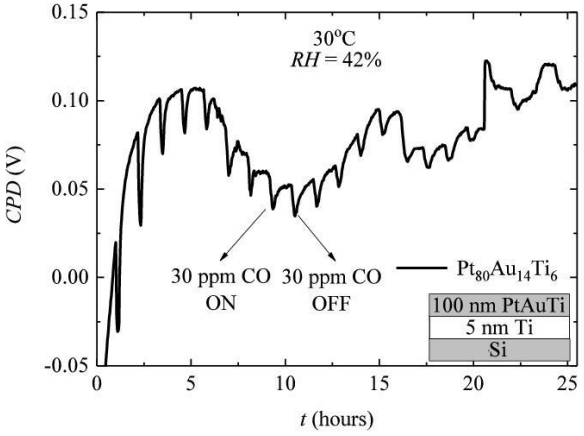

Figure 4. Average of experiment CPD signals from three samples of $Pt_{80}Au_{14}Ti_6$ with 5 nm Ti as adhesive layer to 30 ppm of CO in air with *RH* = 42% at room temperature (30°C) after etched in argon plasma with 300 W, base pressure 5×10^{-2} mbar, and working pressure 2.6×10^{-1} mbar, then measured for 24 hours.

To find the relationship between the concentration of subsurface oxygen and the sticking coefficient of O on Pt, the simulation uses:

1. the original values of all parameters for Pt in Reaction No. 1 – 18, 45, 46 and 61, which have been mentioned in Marjunus (2018) [23],
2. room temperature (30°C),
3. the relative humidity of the chamber (42%),
4. standard pressure (1 atm) of synthetic air (consists of 80% of N_2 and 20% of O_2), and
5. measurement time for 24 hours.

The simulation calculates the amount of O_{chem} and O_{sub} in Mono Layer (ML) with/without considering the surface reaction (adsorption, reaction, and desorption). Considering/not considering the surface reaction are aimed to know whether there is a significant role or not of the surface reaction, or which is responsible for the amount of O_{chem} and O_{sub}. The first result is as given in figure 5.

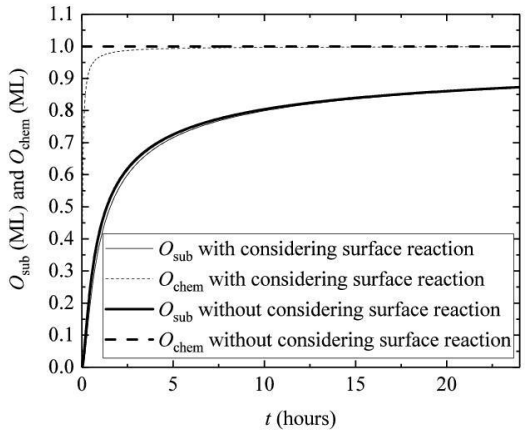

Figure 5. Chemisorbed (O_{chem}) and subsurface oxygen (O_{sub}) on Pt surface with *RH* = 42% at room temperature (30°C) in synthetic air (consists of 80% of N_2 and 20% of O_2), measured for 24 hours,with/without considering the surface reaction.

According to figure 5, by considering the surface reaction, it is shown that at the beginning, $O_2^{(g)}$ will be adsorbed slowly but O_{chem} will reach about 1 ML after 7 hours. It effects to the growing of O_{sub}. On the other hand, without considering the surface reaction, of course, the amount of O_{chem} is perfectly 1 ML started from the beginning. It is looked like that there is no different behavior of O_{sub} with/without considering the surface reaction because the amount of O_{chem} for these two conditions do not also give a big difference. It sounds that the surface reaction does not play a role in the amount of O_{sub}, although its role is intended.

Since figure 5 does not give a clear hint whether the surface reaction plays its role or not for the occupation of O_{sub}, the second simulation has been done as presented in figure 6.

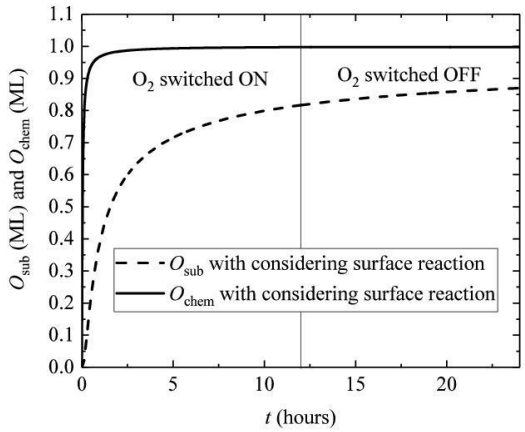

Figure 6. Chemisorbed and subsurface oxygen on Pt surface with *RH* = 42% at room temperature (30°C) in synthetic air (consists of 80% of N_2 and 20% of O_2), exposed by 1 atm of synthetic air for the first 12 hours and in vacuum condition for the last 12 hours, by considering the surface reaction.

In this simulation, Pt surface is exposed by 1 atm of synthetic air for the first 12 hours and conditioned in vacuum for the last 12 hours. This condition was hoped that it can show the role of the surface reaction. Unfortunately, according to the Figure 6, it was hoped, after $O_2^{(g)}$ is switched off, the amount of O_{chem} will decrease automatically which will be followed by decreasing of O_{sub}. This intention finally

cannot be proved. It can be understood, because the huge amount of $O_2^{(g)}$ molecules in the air above the Pt surface and O_{chem} on the surface from the first 12 hours is still enough for covering the Pt surface and diffusing to be O_{sub}. Afterward, since there is still no proof that the surface reaction influences the amount of O_{sub}, the third simulation which is similar to the second simulation has been done. In this simulation, the desorption energy of $2O^{(s)}$ on Pt is used only 10% of its original value [23]. The decreasing of this energy is aimed, that the adsorbed/chemisorbed O on Pt surface is easy to be desorbed. It is hoped, this treatment can show that the surface reaction plays the role of the O_{sub}. Finally, this idea gives the proof that surface reaction especially desorption, controls the amount of O_{sub} as presented in figure 7**.**

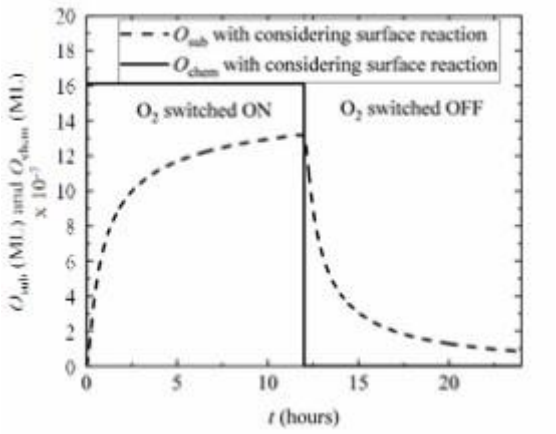

Figure 7. Chemisorbed and subsurface oxygen on Pt surface with *RH* = 42% at room temperature (30ºC) in synthetic air (consists of 80% of N_2 and 20% of O_2, exposed by 1 atm of synthetic air for the first 12 hours and in vacuum condition for the last 12 hours, by considering the surface reaction but using only 10% of desorption energy of $2O^{(s)}$ on Pt.

Afterward, the Signal Attenuation (*SA*) can be formulated as percentage of the signal to the initial signal as revealed in figure 8. Based on figure 8, the trend line of *SA* gives the dependency of *SA* to the time (*t* in hour) with error ($\chi^2 = 0.008$) as written in Equation 30,

$$SA = 0.98343\exp(-0.08981t). \quad (30)$$

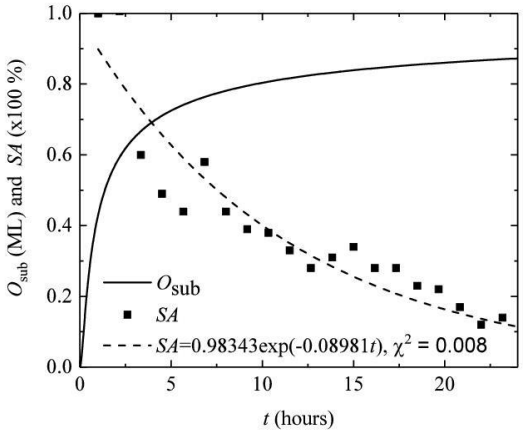

Figure 8. Signal Attenuation (*SA*), its trendline and the increasing of subsurface oxygen (O_{sub}) in 24 hours measurement.

Then, the data of *SA* from these experiments are plotted together with the result from figure 5 which considers the surface reaction, as presented in figure 9.

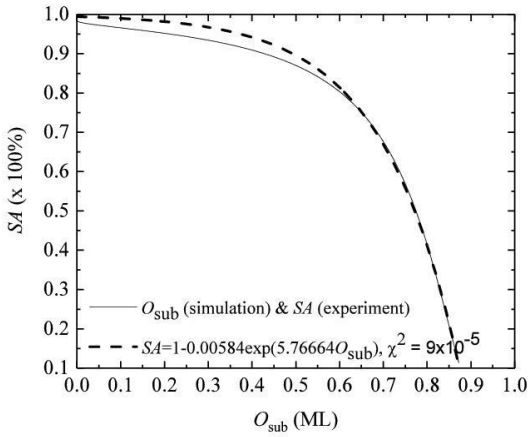

Figure 9. Signal Attenuation (*SA*) versus the increasing of subsurface oxygen (O_{sub}).

According to the figure 9, the relationship between *SA* and O_{sub} is obtained by fitting their data with error ($\chi^2 = 9\times10^{-5}$) as given in Equation 31,

$$SA = 1 - 0.00585\exp(5.76664O_{\mathrm{sub}}). \quad (31)$$

where O_{sub} is the amount of O_{sub}. This relationship (Equation 31) is also called as the adjustment factor for initial sticking coefficient.

Finally, figure 10 presents the comparison of the simulated CPD signal with and without *SA* for loss signal simulation phenomenon on $Pt_{80}Au_{14}Ti_6$ to 30, 60 and 90 ppm CO in air with *RH* = 42% at room temperature (30°C).

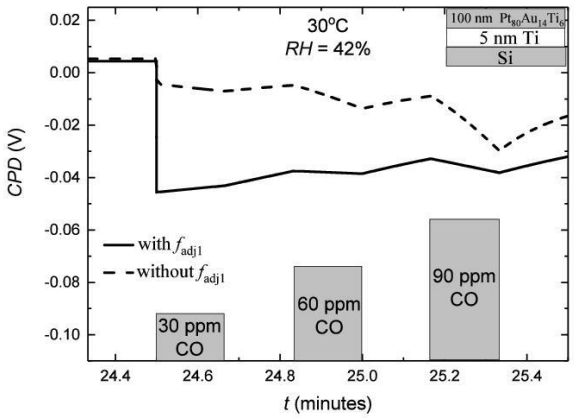

Figure 10. Simulation of loss signal phenomenon with and without *SA* on $Pt_{80}Au_{14}Ti_6$

to 30, 60 and 90 ppm CO in air with *RH* = 42% at room temperature (30°C). From this figure, it can be seen that the signals are not completely vanished after samples are exposed in the air (as experimented results) when simulation does not use *SA*. The simulated CPD signals will be smaller, even almost zero,

when *SA* is employed in the simulation. It proves that *SA* is needed for every sticking coefficient parameter.

4. Conclusions

There is no CPD signals from PtAuTi samples after exposed 24 hours in the air because of oxygen (O) occupation. O can diffuse into Pt (also applied for Au and Ti in simulations) with diffusion constant 10^{-19} cm^2/s forming subsurface oxygen. The process from chemisorbed oxygen to be subsurface oxygen attenuates the sticking coefficient of every gas (O_2, CO, CO_2, H_2O, OH, and H_2) with simulated factor $SA = 1 - 0.00585 \exp(5.76664 O_{\mathrm{sub}})$.

Acknowledgment

The author would like to thank to Ministry of Research and Higher Education, Republic of Indonesia and also to Institut für Physik, Fakultät Elektrotechnik und Informationstechnik, Universität der Bundeswehr München, Germany, for supporting this research.

References

[1] Ernst and Zibrak J D 1998 Carbon monoxide poisoning *J. of Medicine* **339** (22) p 1603–08
[2] Goldstein M 2008 Carbon monoxide poisoning *J. of Emergency Nursing* **34** (6) p 538–42
[3] Senft, Iskra P, Eisele I and Hansch W 2011 Work function - based sensor: Schottky - and FET-based devices (in *Chemical Sensors: Comprehensive Sensor Technologies* ed G Korotchenkov) chap 5 p 180-228
[4] Capone S, Forleo A, Francioso L, Rella R, Siciliano P, Spadavecchia J, Presicce S and Taurino A M 2004 Solid state gas sensors: State of the art and future activities *ChemInform* **35** (29) p 1335-48
[5] Eisele I and Burgmair W 2000 Work function based field effect devices for gas sensing *Proc. Conference on Optoelectronic and Microelectronic Materials and Devices* p 285–91
[6] Friedberger A, Kreisl P, Rose E, Müller G, Kühner G, Wöllenstein J and Böttner H 2003 Micromechanical fabrication of robust low-power metal oxide gas sensors *Sens. Actuators B Chem.* **93** (1-3) p 345–9
[7] Zhou X, Xu Y, Cao Q and Niu S 1997 Metal-semiconductor ohmic contact of SnO_2-based ceramic gas sensors *Sens. Actuators B Chem.* **41** (1-3) p 163–7
[8] Salehi A and Nikfarjam A 2004 Room temperature carbon monoxide sensor using ITO/n-GaAs Schottky contact *Sens. Actuators B Chem.* **101** (3) p 394–400
[9] Kang K S and Lee S P 2003 CO gas sensors operating at room temperature», *J. of Material Scie.* **38** p 4319–23
[10] Ivanovskaya M, Lutynskaya E and Bogdanov P 1998 The influence of molybdenum on the properties of SnO_2 ceramic sensors *Sens. Actuators B Chem.* **48** (1-3) p 387–91
[11] Pohle R, Von S O, Fleischer M, Frerichs H P, Wilbertz Ch and Freund I 2010 Gate pulsed readout of floating gate FET gas sensors *Proc. Engineering* **5**(0) p 3–16
[12] Langmuir I 1922 The mechanism of the catalytic action of platinum in the reactions $CO + O_2 \rightarrow 2CO_2$ and $2H_2 + O_2 \rightarrow 2H_2O$ *Trans. Faraday Soc.* **17** p 621–54
[13] Zimmer M, Burgmair M, Scharnagl K, Karthigeyan A, Doll T and Eisele I 2001 Gold and platinum as ozone sensitive layer in work-function gas sensors *Sens. Actuators B Chem.* **80** (3) p 174–8
[14] Galonska T, Senft C, Widanarto W, Senftleben O, Frerichs H P and Wilbertz Ch 2007 Cross sensitivity and stability of FET - based hydrogen sensors *SENSORS, 2007 IEEE* p 1036-39
[15] Fleischer M, Hoefer U, Pohle R and Stegmeier R 2012 Selective detector for carbon monoxide (US Patent: US2012/0047995 A1)
[16] Lampe U, Simon E, Pohle R, Fleischer M, Meixner H, Frerichs H P, Lehmann M and Kiss G 2005 Gas FET for the detection of reducing gases *Sens. Actuators B Chem.* 111 - 112 p 106 – 10

[17] Leu M, Doll T, Flietner B, Lechner J and Eisele I 1994 Evaluation of gas mixtures with different sensitive layers incorporated in hybrid FET structures *Sens. Actuators B Chem.* **19** (1-3) p 678–81
[18] Kiss G, Várhegyi E B, Mizsei J, Krafcsik O H, Kovács K, Négyesi G, Ostrick B, Meixner H and Réti F Examination 2000 of the CO/Pt/ Cu layer structure with Kelvin probe and XPS analysis *Sens. Actuators B Chem.* **68** (1-3) p 240–3
[19] Bone W A and Andrew G W 1975 Studies upon catalytic combustion. Part I: The union of carbon monoxide and oxygen in contact with a gold surface *Proc. of the Royal Society of London* Series A **109** (751) p 459–76
[20] Ertl G, Neumann M and Streit K M 1977 Chemisorption of CO on the Pt(111) surface *Surface Science* **64** (2) p 393 – 410
[21] Bouwman R and Sachtler W M H 1970 Photoelectric determination of the work function of gold-platinum alloys *J. of Catalysis* **19** (2) p 127–39
[22] Simon S, Marjunus R, Stimpel T, Lindner, Wilbertz Ch, Schmidt I, Wartmann J and Hansch W 2012 Pt/Au based sensor with a PMMA–film for detecting CO in a hydrogen atmosphere», In IMCS 2012 – The 14th *Inter. Meet. on Chem. Sensors* p 327–30
[23] Roniyus M 2018 *Development of Pt-based Sensitive Layer for Carbon Monoxide Work Function Change Based Sensor in Air at Room Temperature* Ph D Thesis (München: Universität der Bundeswehr)
[24] Schmiedl R, Demuth V, Lahnor P, Godehardt H, Bodschwinna Y, Harder C, Hammer L, Strunk H P, Schulz M and Heinz K 1996 Oxygen diffusion through thin Pt films on Si(100) *J. App. Phys* **62** 3 p 223–30
[25] Rotermund H H, Lauterbach J and Haas G 1993 The formation of subsurface oxygen on Pt(100) *J. App. Phys.* **57** 6 p 507–11
[26] Lauterbach J, Asakura K and Rotermund H H 1994 Subsurface oxygen on Pt(100): Kinetics of the transition from chemisorbed to subsurface state and its reaction with CO, H_2 and O_2 *J. Surf. Scie.* **313** 1-2 p 52–63
[27] Callaghan C A 2006 *Kinetics and Catalysis of the Water-Gas-Shift Reaction: A Microkinetic and Graph Theoretic Approach* Ph D Thesis (Worcester: Worcester Polytechnic Institute)
[28] Nix R M 2014 *An Introduction to Surface Chemistry* (London: Queen Mary, University of London)
[29] Yan X T and Xu Y 2010 *Chemical Vapor Deposition* (London: Springer-Verlag)
[30] Somorjai G A and Li Y 2010 *Introduction to Surface Chemistry and Catalysis 2nd Edition* (New York : Wiley & Sons)
[31] Senft C 2009 *Austrittsarbeitsbasierte Wassertofdetektion für Farzeuge mit Brennstoffzellenantrieb* Ph D Thesis (München : Universität der Bundeswehr)
[32] Massman W J 1998 A review of the molecular diffusivities of H_2O, CO_2, CH_4, CO, O_3, SO_2, NH_3, N_2O, NO, and NO_2 in air, O_2 and N_2 near STP Atmospheric Environment **32** (6) p 1111–27